Dual inhibition of MAT2A and PRMT5 delivers synergistic anti-tumor responses in preclinical models of *MTAP*-deleted cancer

Marcus M. Fischer[1], Kimberline Gerrick[1], Brian Belmontes[2], Katherine Slemmons[2], Yevgeniy Freyman[1], Jay Jain[1], Steve Federowicz[1], Isaac Bishof[1], Arjun A. Rao[1], Melissa Fleury[1], Zabrisky Roland[1], Zineb Mounir[1], Mark R. Lackner[1], Paul E. Hughes[2], Mike White[1], Claire L. Neilan[1].

[1]IDEAYA Biosciences, South San Francisco, CA 94080, USA, [2]Amgen Discovery Research, Amgen Inc, Thousand Oaks, CA 91320, USA

AACR Annual Meeting 2023, Poster 1644

Background

- Approximately 15% of all tumors harbor deletions in the 9p21 locus that encompass CDKN2A and MTAP
- In MTAP-deleted tumors, cellular MTA accumulates and partially inhibits the essential protein argenine methyltransferase PRMT5
- This context provides therapeutic opportunities, currently under clinical evaluation, to selectively extinguish PRMT5 activity in tumor cells with MAT2A inhibitors that limit SAM synthesis or with direct PRMT5 inhibitors that are MTA-cooperative
- Here we evaluated the potential benefit of combinatorial pathway suppression with MAT2A and PRMT5 inhibitors in MTAP-WT and MTAP-deleted tumor models in vitro and in vivo

Objective

- To quantitatively assess the consequence of dual inhibition of MAT2A and PRMT5 on MTAP deficient cancer cell and tumor growth
- To determine if this dual inhibition provides additional suppression of PRMT5-mediated protein methylation and target gene expression
- To gain further understanding of the MOA for the MAT2A/PRMT5 dual inhibition by analysis of gene expression patterns and alternative splicing of RNA
- To advance these preclinical findings towards clinical investigation

Introduction

Deletion of the 9p21 tumor suppressor locus confers targetable vulnerabilities in ~15% of all tumor types

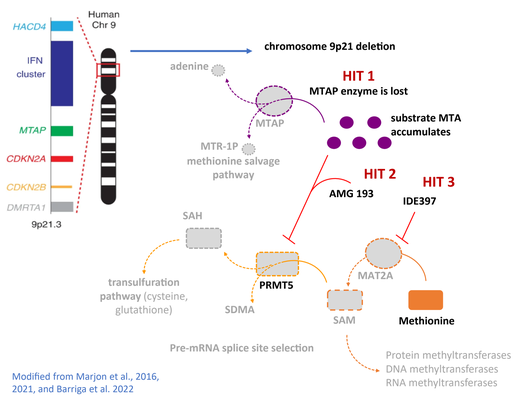

Modified from Marjon et al., 2016, 2021, and Barriga et al. 2022

Baseline SDMA is decreased in *MTAP*-deleted relative to *MTAP*-WT tumors

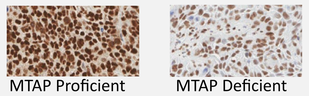

IHC of total SDMA from a PDX model TMA

IDE397 exhibits anti-tumor activity across multiple PDX models; tumor regressions are enriched in histologies where maximal pathway suppression is observed

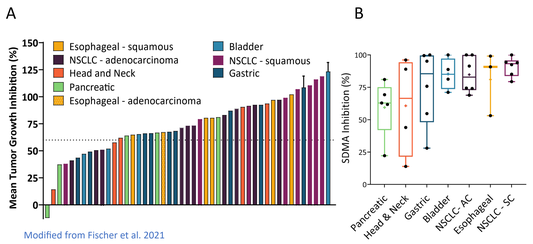

Modified from Fischer et al. 2021

A) 47 MTAP-deleted PDX models were evaluated for anti-tumor response. IDE397 or vehicle was administered at 30 mg/kg/day to 5 mice/group. Mean TGI calculated from final and initial tumor volume. Tumor regression = >100% TGI. **B)** SDMA IHC from tumors isolated from efficacy studies depicted in "A", where available. H-scores were provided by a pathologist and presented as percent inhibition. Each individual model is presented as the mean of 2-3 tumors per treatment group.

Results

Figure 1. Four of eight squamous NSCLC PDX models respond to IDE397 with tumor regressions

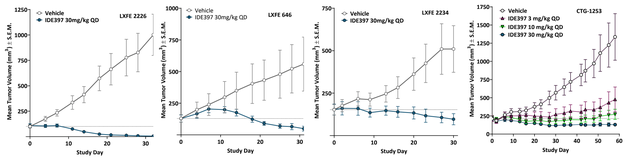

Tumor growth curves for squamous NSCLC PDX models which responded to administration of 30 mg/kg QD IDE397. Tumor samples were collected, where available, from end of study for SDMA IHC and RNAseq. Administration of 30 mg/kg IDE397 produced tumor regressions in these 4 PDX models. Data represent mean ± SEM, 5 mice per group

Figure 2. IDE397 perturbation of mRNA splicing is associated with anti-tumor activity

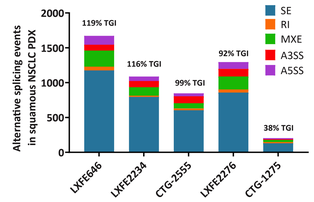

RNAseq with rMATs (v4.1.2) analysis was performed from whole tumor lysate at study termination. Significant AS events as compared to the vehicle group were quantified. Cutoff values for statistical significance were: Absolute difference in Percentage Spliced In ($|dPSI|$) ≥ 0.1, Number of reads supporting the AS event ≥ 10, and False discovery rate (FDR) ≤ 0.05

Figure 3. Baseline methylation pathway suppression observed in MTAP-deleted squamous NSCLC PDX models

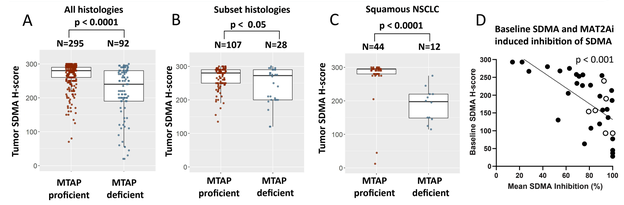

A-C) SDMA IHC from TMAs of treatment naïve PDX models. Statistical significance determined from Mann-Whitney t-test. MTAP status was confirmed by NGS and IHC. **A)** All histologies except squamous NSCLC. **B)** Cholangiocarcinoma, large cell NSCLC, melanoma, and HNSCC. **C)** Squamous NSCLC **D)** Tumor SDMA IHC from PDX models treated with 30 mg/kg/day IDE397. Up to 3 tumors per group were isolated and H-scores determined. Data depicts the mean H-score from the vehicle group (baseline) and % inhibition of SDMA relative to vehicle control. Squamous NSCLC PDX are displayed as open circles.

Figure 4. Enhanced anti-tumor response achieved with IDE397 in combination with MTA-cooperative PRMT5i

MTA-cooperative PRMT5 inhibitor demonstrates MTA-cooperativity

MTA-cooperative PRMT5i combined with IDE397 is synergistic in MTAP-/-

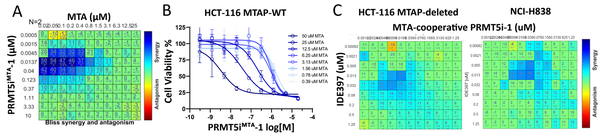

Combination of MAT2A inhibitor IDE397 + MTA-cooperative PRMT5 inhibitors produces enhanced anti-tumor response in MTAP-deleted tumor models

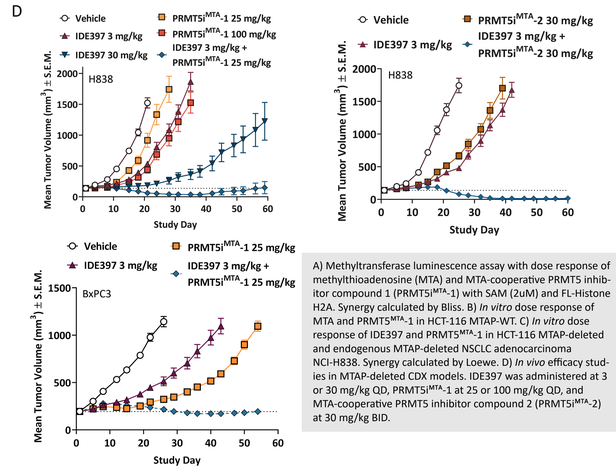

A) Methyltransferase luminescence assay with dose response of methylthioadenosine (MTA) and MTA-cooperative PRMT5 inhibitor compound 1 (PRMT5iMTA-1) with SAM (2uM) and FL-Histone H2A. Synergy calculated by Bliss. B) *In vitro* dose response of MTA and PRMT5iMTA-1 in HCT-116 MTAP-WT. C) *In vitro* dose response of IDE397 and PRMT5iMTA-1 in HCT-116 MTAP-deleted and endogenous MTAP-deleted NSCLC adenocarcinoma NCI-H838. Synergy calculated by Loewe. D) *In vivo* efficacy studies in MTAP-deleted CDX models. IDE397 was administered at 3 or 30 mg/kg QD, PRMT5iMTA-1 at 25 or 100 mg/kg QD, and MTA-cooperative PRMT5 inhibitor compound 2 (PRMT5iMTA-2) at 30 mg/kg BID.

Figure 5. MTAP-deletion is sufficient to confer enhanced anti-tumor response to the IDE397+PRMT5i combination

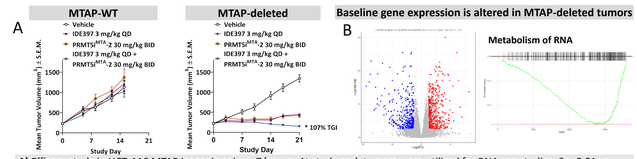

A) Efficacy study in HCT-116 MTAP isogenic pair, n=7/group. At study end, tumors were utilized for RNA seq studies. *p<0.01 vs monotherapy, 2-way RM ANOVA with Tukey's post-test. **B)** Analysis of differential gene expression between HCT-116 MTAP-deleted vs. MTAP-WT from the vehicle group. Volcano plot shows significant differentially expressed genes. Gene set enrichment analysis (GSEA) revealed multiple gene sets differentially impacted in MTAP-deleted tumors, including those involved in RNA metabolism.

Figure 6. The combination effect in MTAP-deleted tumors is predominantly a deepening of monotherapy activity

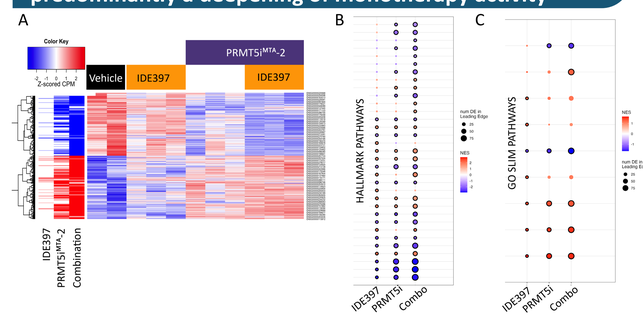

RNAseq analysis from HCT-116 MTAP-deleted study depicted in Figure 5A. **A)** Heatmap of Z-scored TMM-normalized Counts Per Million **B)** Enrichment of Hallmark Pathways from MSigDB. **C)** Enrichment of GO Slim set. **(B and C)** The color of each spot describes the Normalized Enrichment Score (NES) and the shape describes the number of genes in the Leading Edge that are significantly, differentially regulated. Spots with a black border were statistically significant (P.adj < 0.05).

Figure 7. Tumor SDMA modulation is deeper and more durable in combination compared to monotherapy

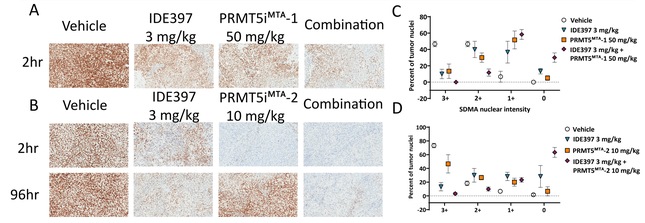

A) Representative SDMA IHC images from HCT-116 MTAP-deleted CDX following administration of IDE397 3 mg/kg QD, Compound 1 at 50 mg/kg QD, or the combination, 2hrs post-dose on Day 2. **B)** NCI-H838 CDX following administration of IDE397 3 mg/kg QD, Compound 2 at 10 mg/kg BID, or the combination for 7 days. Tumors were isolated at 2hrs or 96hrs post the final dose. **C)** Distribution of SDMA positive tumor nuclei from "A". **D)** Distribution of SDMA positive tumor nuclei from "B" at 96hr. 3+ strong positive, 2+ moderate positive, 1+ weak positive, 0 negative for nuclear SDMA. Images are 20x magnification.

Figure 8. Quantitative assessment of drug effects on pre-mRNA splicing fidelity reveals a stronger disruption with combination treatments

A **Treatment enriched alternative splicing in MTAP-deleted tumors**

B **Distribution of alternative splicing between groups in MTAP-deleted**

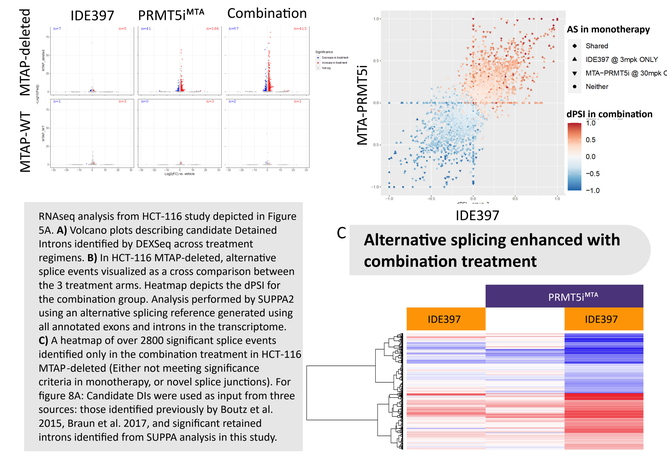

RNAseq analysis from HCT-116 study depicted in Figure 5A. **A)** Volcano plots describing candidate Detained Introns identified by DEXSeq across treatment regimens. **B)** In HCT-116 MTAP-deleted, alternative splice events visualized as a cross comparison between the 3 treatment arms. Heatmap depicts the dPSI for the combination group. Analysis performed by SUPPA2 using an alternative splicing reference generated using all annotated exons and introns in the transcriptome. **C)** A heatmap of over 2800 significant splice events identified only in the combination treatment in HCT-116 MTAP-deleted (Either not meeting significance criteria in monotherapy, or novel splice junctions). For figure 8A: Candidate DIs were used as input from three sources: those identified previously by Boutz et al. 2015, Braun et al. 2017, and significant retained introns identified from SUPPA analysis in this study.

Figure 9. Combinatorial PRMT5 pathway inhibition with the clinical compounds AMG 193 and IDE397 recapitulates synergy and produces durable efficacy at well tolerated doses

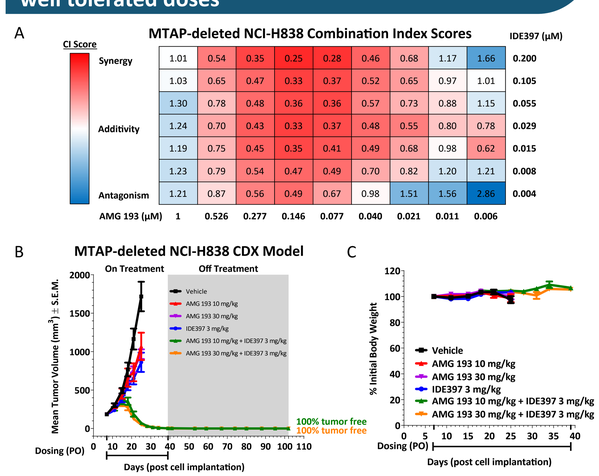

A) H838 NSCLC cell line was treated with a combination of MTA-cooperative PRMT5 inhibitor AMG 193 and IDE397 in an 8 x 10 dose matrix including DMSO-only controls. Cell viability was measured by the CellTiter-Glo Luminescence assay after 6 days of treatment. CalcuSyn software was used to generate Combination Index (CI) scores to assess synergy, shown on heatmap. CI<1 indicates synergy. C=1 indicates additivity. C>1 indicates antagonism. B) Female nude mice were implanted with H838 (NSCLC CDX) tumors. Vehicle, AMG 193, and IDE-397 were administered orally (PO) once a day for a total of 33 doses. Data represent mean ± SEM, n = 10 for each group. Off treatment observation phase (grey shaded) used to assess durability of response. Animals with no measurable tumor were classified as tumor free. C) Body weight change from "B"

Conclusions

1. Synergistic antiproliferative effects were observed when the potent and selective MAT2A inhibitor IDE397 was combined with any of multiple MTA-cooperative PRMT5 inhibitors in MTAP-deleted cell lines in vitro
2. In vivo, the combination of IDE397 and MTA-cooperative PRMT5 inhibitors were well tolerated, and induced durable tumor regressions, including complete responses, at dose levels below the maximally efficacious preclinical dose of each individual agent
3. Pharmacodynamic target engagement in the tumor was evaluated by quantitative assessment of symmetric dimethyl arginine (SDMA) and indicated greater extent of PRMT5 inhibition by combination treatment as compared to either agent alone
4. Combined inhibition of MAT2A and PRMT5 appears to largely amplify the biological affects of each single agent suggesting synergistic efficacy occurs via maximal SDMA pathway suppression in MTAP-deleted cancers
5. Modulating PRMT5 activity through 2 distinct nodes offers a compelling dual synthetic lethal opportunity to address unmet need for the many patients afflicted with MTAP-deleted cancers
6. IDEAYA Biosciences and Amgen have entered into a clinical trial collaboration agreement to assess the combination of IDE397 and AMG 193 in a Phase 1 clinical trial.

Acknowledgements

1. Pharmaron, Charles River, Wuxi Apptec, Champions Oncology, Xentech, and Crown Biosciences for performing in vivo studies
2. HudsonAlpha Discovery for RNA sequencing
3. Fios Genomics and Directed Bio for gene expression and splicing analysis
4. Mosaic Laboratories for SDMA IHC analysis
5. Jeanne Quirit, Till Maurer, Alex Embusch, and Peter Teriete for in vitro assessment of MTA-cooperativity.

References

1. Fischer MM, Bhola N, Faulhaber J, Freyman Y, Yao B, Mounir Z, et al. Abstract 1278: MAT2A inhibitor, IDE397, displays broad anti-tumor activity across a panel of MTAP-deleted patient-derived xenografts. Cancer Research. 2021;81:1278–1278.
2. Marjon K, Cameron MJ, Quang P, Clasquin MF, Mandley E, Kunii K, et al. MTAP Deletions in Cancer Create Vulnerability to Targeting of the MAT2A/PRMT5/RIOK1 Axis. Cell Reports. 2016;15:574–87.
3. Marjon K, Kalev P, Marks K. Cancer Dependencies: PRMT5 and MAT2A in MTAP/p16-Deleted Cancers. 2020;20.
4. Barriga FM, Tsanov KM, Ho Y-J, Sohail N, Zhang A, Baslan T, et al. MACHETE identifies interferon-encompassing chromosome 9p21.3 deletions as mediators of immune evasion and metastasis. Nat Cancer. 2022;3:1367–85.
5. Boutz PL, Bhutkar A, Sharp PA. Detained introns are a novel, widespread class of post-transcriptionally spliced introns. Genes Dev. 2015;29:63–80.
6. Braun CJ, Stanciu M, Boutz PL, Patterson JC, Calligaris D, Higuchi F, et al. Coordinated Splicing of Regulatory Detained Introns within Oncogenic Transcripts Creates an Exploitable Vulnerability in Malignant Glioma. Cancer Cell. 2017;32:411-426.e11.